Materials Letters 225 (2018) 54–56

Contents lists available at ScienceDirect

Materials Letters

journal homepage: www.elsevier.com/locate/mlblue

Surface scattering effect on the electrical mobility of ultrathin Ce doped In_2O_3 film prepared at low temperature

Jianhua Shi [a,b], Fanying Meng [a,b,*], Jian Bao [c], Yongwu Liu [a,b], Zhengxin Liu [a,b]

[a] Research Center for New Energy Technology, Shanghai Institute of Microsystem and Information Technology (SIMIT), Chinese Academy of Sciences (CAS), 235 Chengbei Rd, Jiading, 201800 Shanghai, PR China
[b] University of Chinese Academy of Sciences (UCAS), Shijingshan, 100049 Beijing PR China
[c] Trina Solar Co., Ltd, Changzhou, Jiangsu 213031, PR China

ARTICLE INFO

Article history:
Received 19 March 2018
Received in revised form 17 April 2018
Accepted 25 April 2018
Available online 26 April 2018

Keywords:
Ultrathin
High mobility
ICO
Surface scattering

ABSTRACT

Electrical conduction behavior of ultrathin cerium doped In_2O_3 (ICO) films fabricated by reactive plasma deposition (RPD) method at low temperature is investigated. It is found that both carrier density and mobility of ICO film are dependent on the film thickness strongly. When the film thickness is increased from 5 nm to 300 nm, carrier density improved gradually from 0.5×10^{20} cm^{-3} to 2.1×10^{20} cm^{-3}, while carrier mobility increased from 35.1 cm^2/Vs to 153.7 cm^2/Vs and then decreased slightly to 121.5 cm^2/Vs. The limited carrier mobility is theoretically discussed from analyzing the counterplay between grains boundary scattering-limited and surface scattering-limited mechanism.

1. Introduction

Transparent conducting oxide (TCO) films are widely used as transparency electrodes in photoelectronic devices because of their low electrical resistivity and high transmittance from visible to near-IR regions of the optical spectrum [1,2]. In particular, ultrathin TCO films (<50 nm) with resistivity of $\sim 10^{-4}$ Ω cm are intensely required to achieve thinner, larger, flexible and higher performance [3,4]. Unfortunately, electrical conductivity of thin TCO films deteriorate rapidly due to their few tens nanometer "dead layer" at the initial growth stage [5,6]. Until now, based on the improvement crystalline of ultrathin TCO film using advanced deposition methods, 30 nm thick tin doped indium oxide (ITO) [7], 30 nm thick gallium doped zinc oxide (GZO) [8] and 20 nm thick aluminum doped zinc oxide (AZO) [9] with low resistivity ($<5 \times 10^{-4}$ Ω cm) have been prepared. Actually, it was reported that when the film thickness of TCO film is comparable with bulk mean free path of electron, size effects on electrical conductivity should be considered seriously [10,11]. In this letter, we prepared cerium doped indium oxide (ICO) films with various film thicknesses from 5 nm to 300 nm using reactive plasma deposition (RPD) method and the carrier transport properties are theoretically discussed.

2. Experimental

The ICO films are deposited on intention heated quartz substrates using RPD method. The details concerning the RPD technique is described elsewhere [8]. The source material of ICO films is 3 wt% CeO_2 doped In_2O_3 and oxygen partial pressure is set at about 1×10^{-4} Torr for achieving high quality films as revealed in our previous study [12] The substrate carrier speed is varied from 2 to 200 mm/min to modulate the thickness of ICO films. The thickness of ICO films is confirmed by variable angle spectroscopic ellipsometry (VASE J.A Woolam M-2000XI) measurement. The electrical properties are determined by Hall effect in the Van der Pauw configuration measurement system (Ecopia HMS-5000). The surface morphologies of the films are characterized by an atomic force microscopy (AFM. Bruker Dimension FastScan) while the structure of films is analyzed by grazing incidence X-ray diffraction (GIXRD. Bruker D8 Discover).

3. Results and discussion

The carrier mobility (μ), carrier density (n) and electrical resistivity (ρ) of ICO thin films are showed in Table 1. For the ultrathin ICO films (<50 nm), both the n and μ decrease rapidly with thinning the film thickness, from 1.9×10^{20} to 0.5×10^{20} cm^{-3}, and 153.7 to 35.1 cm^2/Vs, respectively. Therefore, the ρ value increase greatly from 2.2×10^{-4} to 37×10^{-4} Ω cm. Nevertheless, the

* Corresponding author at: Research Center for New Energy Technology, Shanghai Institute of Microsystem and Information Technology (SIMIT), Chinese Academy of Sciences (CAS), 235 Chengbei Rd, Jiading, 201800 Shanghai, PR China.
E-mail address: fymeng@mail.sim.ac.cn (F. Meng).

https://doi.org/10.1016/j.matlet.2018.04.102
0167-577X/

Table 1
Electrical properties of ICO films as a function of film thickness.

Film thickness (nm)	Carrier density ($\times 10^{20}$ cm^{-3})	Resistivity ($\times 10^{-4}$ Ω cm)	Carrier mobility (cm^2/Vs)
5	0.5	37	35.1
10	0.9	15	45.7
20	1.7	2.5	124.9
30	1.9	2.2	153.7
50	2.0	2.0	150.5
100	2.1	2.1	133.8
150	2.1	2.4	125.8
300	2.1	2.4	121.5

n keeps almost constant at about 2.1×10^{20} cm^{-3} while the μ decreases gradually to 121.5 cm^2/Vs when further increasing the film thickness from 50 to 300 nm.

Based on measurements and fits data, the thickness of "dead layer" (δd) is calculated to be only about 1.0 nm by fitting of sheet carrier density (n_s) to film thickness (d) [13], as showed in Fig. 1. It has been reported [13] that n is independence of film thickness as long as d > δd. In our cases, however, the n value decreases gradually with decreasing the film thickness from 50 nm to 10 nm in despite of d ≫ δd. That is to say, "dead layer" is no longer a well explain for the poor electrical properties in ultrathin ICO films. In order to further know the structure of ultrathin ICO films, typical atomic force microscopy (AFM) images of 10 nm and 300 nm thick ICO film have been presented in the inset image of Fig. 1 as well. All grains in film are irregular and compactly connected to one another. The room-mean-square (R_{ms}) roughness is 0.5 nm and 0.7 nm within a 2×2 μm^2 area, respectively. In fact, smoother surface could be achieved by manipulating the initial film growth mode, as discussed in our previous work [12].

Fig. 2 shows the GIXRD curves of ICO films with various film thickness. A main diffraction peak of 2theta = 32.89° is observed for the 10 nm and 20 nm thick film, corresponding to the (1 2 3) plane of In_2O_3 powder (JCPDS No.06-0416). With increasing the film thickness to 50 nm, the intensity of (1 2 3) diffraction peak increases, and another strong diffraction peak at 2theta = 30.53° corresponding to the (1 1 1) plane appears. However, the (1 1 1) orientation disappeared in thicker films (>100 nm). Therefore, the texture of ICO films is dependent on film thickness greatly, consisting with the ITO film properties deposited by sputtering very well [14]. The mean grain sizes (g) deduced from main XRD diffraction

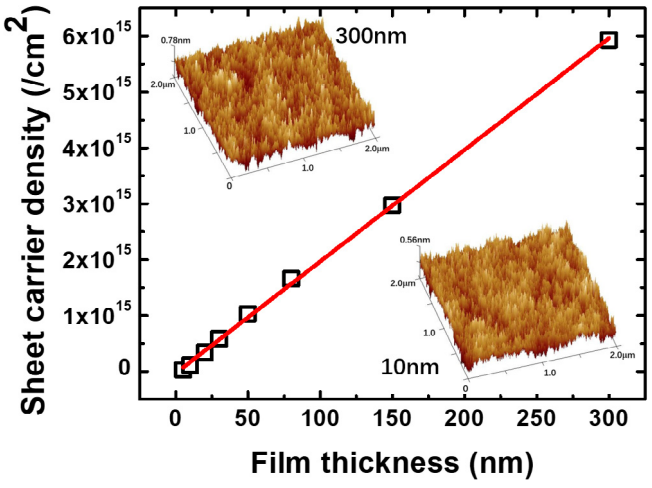

Fig. 1. A least-squares line fit sheet carrier density (N_s) for ICO films of various film thickness (d) using the relationship $N_s = N_b(d-\delta d)$. The AFM images of the 10 nm and 300 nm thick ICO film are also showed in inset.

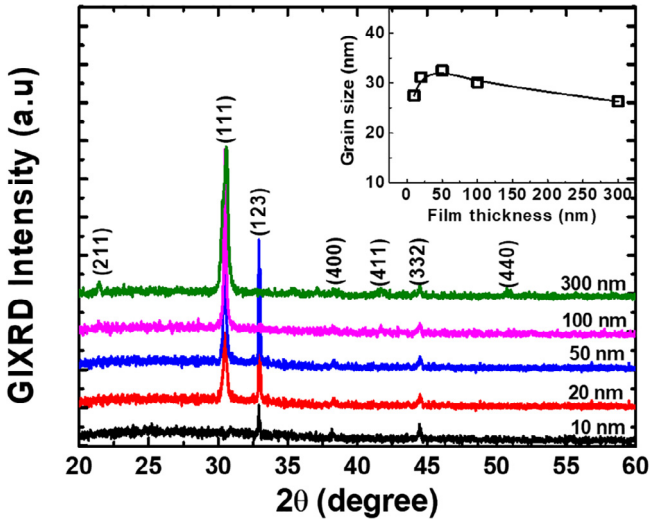

Fig. 2. Typical XRD patterns of ICO with various film thicknesses. The mean grain sizes derive from Scherrer equation are presented in inset image as well.

peak increases firstly from 28 nm to 32 nm and then decreases to around 26 nm with increasing the film thickness, as showed in inset of Fig. 2. Regarding their excellent crystalline, the lower mobility of ultrathin ICO films (<30 nm) can't even be simply attributed to grain boundary, ionized impurities, phonons, or neutral impurities [15].

The effect of surface scattering on carrier mobility is studied according to Fuchs-Sondheimer theory and Many model [16,17], which is applied to understand the nature of scattering mechanism in polycrystalline semiconductors. However, there appears to be very little clear experimental evidence for surface scattering due to the poor crystallinity of these thin semiconductor films. In our case, the total mobility (μ_{total}) is evaluated in terms of grain boundary scattering-limited mobility (μ_{gb}) and surface scattering-limited mobility (μ_{ss}) by invoking Mathiessen's rule as following [18]:

$$1/\mu_{total} = 1/\mu_{gb} + 1/\mu_{ss} \quad (1)$$

In which,

$$\mu_{gb} = \mu_o[1 - 1.5\alpha + 3\alpha^2 - 3\alpha^3 ln(1 + \alpha^{-1})] \quad (2)$$

$$\alpha = (L/g)[R/(1 - R)] \quad (3)$$

$$\mu_{ss} = \mu_o[1/(1 + 2L/d)] \quad (4)$$

$$L = \mu_o(kTm^*/2\pi q^2)^{1/2} \quad (5)$$

where, μ_o is the bulk mobility, L is mean free path of bulk electron, g is the mean grain size, R is the fraction of the electrons, d is the film thickness, k is the Boltzmann constant, T is the temperature, m^* is the electron effective mass and q is the elementary charge. To simplify this theoretical calculation, we assume that the value of μ_o is 1300 cm^2/Vs, which is the maximum value of mobility in high crystal quality In_2O_3 [19]. Therefore, the L is calculated to be about 27 nm using the Eq. (5). The variation of mobility with grain size and film thickness according to Matthiessen's rule is showed in Fig. 3. According to the theoretical fitting results from Eqs. (2) and (4), the μ_{ss} decrease sharply from 1200 cm^2/Vs to 350 cm^2/Vs (data not show here) as the film thickness is reduced from 300 nm to 10 nm. However, the μ_{gb} keeps almost constant due to their small varied mean grain sizes. That is to say, carrier mobility is dominated by the surface scattering-limited mechanism for the ultrathin ICO film (<30 nm), the thinner the film thickness, the lower the carrier

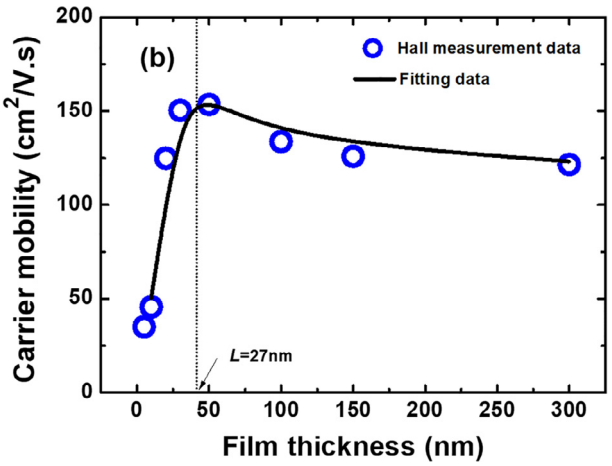

Fig. 3. The simulated carrier transport mobility results of ICO film, circle stands for experimental mobility and the solid line indicates fitted values ($1/\mu_{total=1}/\mu_{gb+1}/\mu_{ss}$) obtained by least-squares fitting.

mobility. This result proves an experimentally powerful evidence for carrier transport being limited by electron surface scattering in polycrystalline semiconductor thin films. On the contrary, carrier mobility is governed by grain boundary scattering-limited mechanism if the film thickness is thicker than 50 nm. Therefore, it is a challenge to achieve high carrier mobility in ultrathin TCO film by intentional improving the thin film's crystallinity.

4. Summary

In conclusion, high mobility ICO films are prepared using RPD method. The dependence of structural and electrical properties of ICO films on thickness are investigated. The preferred orientation transformation is occurred when the thickness of ICO film is increased from 10 nm to 20 nm. Correspondingly, the carrier mobility enlarged abruptly from 45.7 cm^2/Vs to 124.9 cm^2/Vs, even maximize to 153.7 cm^2/Vs at the thickness of 30 nm and then decline to 121.5 cm^2/Vs when the film thickness is 300 nm. Furthermore, it is found that the carrier mobility is dominated by the electron surface scattering-limited mechanism when the film thickness is less or comparable to the mean free path of electron. Thanks to its ultrathin and excellent electrical properties, conversion efficiency over 23.5% in the industrial silicon heterojunction solar cells is possible in the near future based on our previous 23.1% silicon heterojunction solar cell [20]. Furthermore, the ultrathin ICO film is a promising candidate transparent conductive material in other advanced photoelectronic devices.

Acknowledgements

This work was supported by the Main Direction Program of Knowledge Innovation of Chinese Academy of Sciences (No. KGCX2-YW-399+11), International S&T Cooperation Program of China (No. 2015DFA60570) and China Natural Science Foundation of Jiangsu Province (No. BK20161202).

References

[1] K. Ellmer, Nat. Photonics 6 (2012) 809.
[2] U. Betz, M.K. Olsson, J. Marthy, M.F. Escolá, F. Atamny, Surf. Coat. Technol. 200 (2006) 5751.
[3] S. Kang, S. Cho, P. Song, Thin Solid Films 559 (2014) 92–95.
[4] E.J. Guo, H.B. Lu, M. He, K.J. Jin, G.Z. Yang, Appl. Optics 49 (2010) 5678.
[5] X.W. Sun, H.C. Huang, H.S. Kwok, Appl. Phys. Lett. 68 (1996) 2663.
[6] E.J. Guo, H.Z. Guo, H.B. Lu, K.J. Jin, M. He, G.Z. Yang, Appl. Phys. Lett. 98 (2011) 011905.
[7] S.M. Wie, C.H. Hong, S.K. Oh, W.S. Cheong, Y.J. Yoon, J.S. Kwak, Ceram. Int. 40 (2014) 11163.
[8] T. Yamada, T. Nebiki, S. Kishimoto, H. Makino, K. Awai, T. Narusawa, T. Yamamoto, Superlattices Microstruct. 42 (2007) 68–73.
[9] A. Suzuki, M. Nakamura, R. Michihata, T. Aoki, T. Matsushita, M. Okuda, Thin Solid Films 517 (2008) 1478–1481.
[10] Y.J. Zhang, K.H. Gao, Z.Q. Li, Appl. Phys. Lett. 106 (2015) 101602.
[11] J.P. Niemelä, Y. Hirose, T. Hasegawa, M. Karppinen, Appl. Phys. Lett. 106 (2015) 042101.
[12] J.H. Shi, L.L. Shen, F.Y. Meng, Z.X. Liu, Mater. Lett. 182 (2016) 32–35.
[13] D.C. Look, Mater. Sci. Semicond. Process. 69 (2017) 2.
[14] Y.S. Jung, S.S. Lee, J. Cryst. Growth 259 (2003) 343.
[15] K. Ellmer, R. Mientus, Thin Solid Films 516 (2008) 4620.
[16] E.H. Sondheimer, Adv. Phys. 50 (6) (2001) 499.
[17] A. Many, Y. Goldstein, N.B. Grover, in: Semiconductor Surface, North-Holland, Amsterdam, 1965, pp. 307–308.
[18] H.H. Wieder, Jour. Vac. Sci. Technol. 9 (1972) 1193.
[19] O. Bierwagen, J.S. Speck, Appl. Phys. Lett. 97 (2010) 072103.
[20] F.Y. Meng, J.N. Liu, L.L. Shen, J.H. Shi, A.J. Han, L.P. Zhang, Y.C. Liu, J. Yu, J.K. Zhang, R. Zhou, Z.X. Liu, Front. Energy 11 (1) (2017) 78–84.